JOURNAL OF MATERIALS SCIENCE **39** (2004) 235–240

Gadolinia doped ceria/yttria stabilised zirconia electrolytes for solid oxide fuel cell applications

J. LUO, R. J. BALL*, R. STEVENS
Materials Research Centre, Department of Engineering and Applied Science, University of Bath, Bath, BA2 7AY, UK
E-mail: richard.ball@bristol.ac.uk
E-mail: r.stevens@bath.ac.uk

Solid oxide fuel cells are currently constructed using a yttria stabilised zirconia electrolyte membrane. However, zirconia has a number of disadvantages associated with its use, such as the high operational temperatures required for it to exhibit acceptable levels of ionic conductivity. Alternative ceramics such as doped cerium oxide show promise as electrolytes capable of operating at reduced temperatures, but introduce additional problems such as electronic conduction and inferior mechanical properties. This paper describes the manufacture and characterisation of a number of prototype electrolytes consisting of a mixture of yttria stabilised zirconia and gadolinium doped ceria. Traditional ceramic processing techniques were used to produce the samples, which were then examined using dilatometry, impedance spectroscopy and X-ray diffraction. Results show a lowering of the ionic conductivity of zirconia with the addition of doped ceria. X-ray diffraction patterns obtained from the samples suggested that this effect could be attributed to the formation of a solid solution of ceria in zirconia.

1. Introduction

As requirements for cheap clean electrical energy grow, fuel cells are becoming an increasingly viable source of power for many application. There are a number of different fuel cell systems currently available on the market such as proton exchange membrane (PEM), alkaline electrolyte and high temperature fuel cells, each of which operates at varying temperatures and efficiencies. The solid oxide fuel cell (SOFC) is classed as a high temperature cell and has an operational temperature in the region of 1000°C. During operation of a SOFC heat is generated in addition to electricity. Modern fuel cells commonly use the excess heat generated to produce more electricity or heat water for commercial or residential applications. This versatility allows very high fuel efficiencies to be obtained and has lead to the commercial success of the solid oxide fuel cell over alternative designs.

During the operation of a SOFC, oxygen gas on the cathode side of the cell combines with electrons to produce two O^{2-} ions. These subsequently diffuse through the electrolyte layer and combine with the fuel producing electricity and heat.

Fuel cell efficiency can be dependant on the properties of the materials from which the cell is fabricated. One of the more critical components in the fuel cell is the solid electrolyte. Electrolytes must have high oxygen ion conductivity at the operating temperature to allow efficient transfer of ions from the cathode to the anode, but also a low electronic conductivity to prevent electron leakage across the cell. In addition the electrolyte must be gas tight to prevent diffusion of either oxygen gas or fuel. Should any of these properties deteriorate during operation, a reduction in efficiency, followed by cell failure, is the result.

Tetragonal or cubic yttria stabilised zirconia (YSZ) is the most common electrolyte used in commercial SOFC's [1, 2]. It is stable in both the reducing and oxidising atmospheres of the anode and cathode and exhibits a high ionic conductivity of 0.1 S cm^{-1} at the operating temperature of 1000°C. In addition tetragonal YSZ has good mechanical properties with a room temperature strength and toughness of 1000 MPa [3] and 7–10 MPam [1, 2, 4] respectively. Electronic conductivity is negligible at the oxygen partial pressures within the fuel cell. Nevertheless, the great disadvantage of YSZ is that a high operating temperature of $\approx$1000°C is necessary to achieve the high level of ionic conductivity required for efficient operation.

YSZ electrolyte fuel cells utilise interconnectsformed from nickel chromium alloys that are able to withstand the high operational temperatures. However, these alloys contribute to a significant proportion of the total fuel cell cost. Electrolyte materials, which exhibit similar properties to zirconia, at lower temperatures, would allow interconnects to be constructed of cheaper stainless steel components, considerably reducing the overall manufacturing costs.

*Present address: Interface Analysis Centre, University of Bristol, Bristol, BS2 8BS, UK.

Doped cerium oxide has a higher ionic conductivity compared to the currently used zirconia and is an attractive choice as a replacement electrolyte. When the cerium oxide fluorite related structure is doped with lower valent cations, such as Gd^{3+}, anion vacancies are created. These vacancies allow the diffusion of oxygen ion's through the structure. Calculations have shown that the conductivity can be optimised when the ionic radius of the substituting ion matches that of the host ion, as is the case for gadolinium in ceria.

However, a number of disadvantages are associated with the use of gadolinium doped ceria. It not only has a significantly lower strength of 140–180 MPa [5, 6] compared to that of zirconia, but is also less stable at the oxygen partial pressures present during fuel cell operation. Increased electronic conductivity arising due to defect oxide formation can produce a lower cell potential, thus reducing efficiency.

This paper describes the manufacture and characterisation of a number of composite electrolytes consisting of various ratios of gadolinia doped ceria ($Ce_{0.9}Gd_{0.1}O_{1.95}$) and 3% yttria stabilised zirconia (3Y-TZP).

2. Experimental methods

2.1. Sample processing

The compositions produced are shown in Table I. All samples were manufactured using traditional ceramic processing methods with binders such as polyethylene glycol (PEG) added to improve green body formation where necessary. The oxide powders were first wet milled in isopropanol prior to uniaxial and cold isostatic pressing at 100 MPa. Sintering of the green bodies was conducted over a temperature range of 1400 to 1600°C for 3–8 h. The maximum density obtained for the samples was 93% of the theoretical density.

2.2. Dilatometry

Thermal expansion coefficients of the sintered samples for each composition were measured using a Netsch dilatometer. Experiments were conducted in an atmosphere of air using an alumina sample holder. Measurements of expansion were taken in the range of 200 and 900°C using a ramp rate of 3°C min^{-1}. Plots of percentage change in length versus temperature were constructed for each of the samples tested.

2.3. Impedance spectroscopy

The use of impedance spectroscopy to determine the ionic conductivity in zirconia ceramics was first introduced by Bauerle in 1969 [7]. SOFC electrolytes are oxygen ion conductors and can therefore be studied using this technique. Impedance spectroscopy is essentially a non-destructive technique that can provide information that cannot be obtained by other means. It is particularly useful for the study of mobile charges in ionic, semi-conducting or insulating solids [8] and is able to measure the resistance, more correctly the impedance, of the grain boundary, the grain and the electrode of a sample.

Sample properties were measured using a Solartron dielectric test system. This consists of a Solarton FRA model 1260 frequency response analyser coupled with a 1296 dielectric interface. The PC based 'Solartron Impedance Measurement Software Version 2.0.0' was used to interpret the data. Each set of measurements was taken over a frequency range of 0.5 Hz to 2 MHz.

In order to obtain values for the activation energy for ionic conduction a measurement of the frequency response of each sample is required over a range of different temperatures. This was achieved using a specially adapted tube furnace containing a recrystallised alumina sample holder. Platinum paste was applied to each side of the samples, which was subsequently sintered, producing solid platinum electrodes. When placed in the sample holder a spring loaded connection to the platinum contact allowed a circuit to be made between the sample and dielectric interface. Measurements were repeated over a range of temperatures between 200 and 450°C.

A complex plane plot, real impedance, Z', versus imaginary impedance, Z'', was produced for each set of data. On curve fitting a circle to semicircles on these plots, sample resistance, R, can be obtained. The conductivity, σ, was then calculated from the resistance, cross-sectional area, A, and thickness, 1, using Equation 1.

$$\sigma = \frac{l}{R \cdot A} \tag{1}$$

The process enthalpy, ΔH_σ, can be related to conductivity, temperature, T, Boltzmann's constant, k, and a pre-exponential factor, A_σ, using Equation 2.

$$\sigma T = A_\sigma \exp\left[\frac{-\Delta H_\sigma}{kT}\right] \tag{2}$$

The true activation energy for charge migration is included in the process enthalpy in addition to associate energy terms for defect formation [9]. The equation may be linearised by plotting a logarithmic relationship between $\ln(\sigma T)$ and $1/T$, allowing the process enthalpy to be obtained from the gradient of the line of best fit of data plotted using these values.

TABLE I Composition of samples tested

Sample	wt% 3Y-TZP	Wt% cerium gadolinium oxide
TZ3Y	100	0
T-10CG	90	10
T-30CG	70	30
T-50CG	50	50
CG	0	100

2.4. X-ray diffraction

X-ray diffraction (XRD) is a convenient method to obtain crystallographic information about a sample. Diffraction patterns were produced using a Philips PW1730/00 diffractometer with radiation of wavelength, λ, 1.5405 Å (Copper K_α). Scanning was carried

out over a 2-theta range of 25–75 degrees with a step size of 0.010 degrees and scan speed of 0.5 s per step.

The lattice spacing, d, for specific planes (hkl), in each sample were calculated using the Braggs law, Equation 3. Lattice parameters (a, b, c) were then calculated using Equation 4.

$$n\lambda = 2d \sin\theta \tag{3}$$

$$\frac{1}{d^2} = \frac{h^2}{a^2} + \frac{k^2}{b^2} + \frac{l^2}{c^2} \tag{4}$$

3. Results and discussion

Plots of thermal expansion ($\mathrm{d}L/L$) versus temperature of the monolithic and composite materials are given in Fig. 1. Correlation coefficients of linear trend lines fitted to the data were all 0.998 or greater, suggesting strongly that the relationship between thermal expansion and temperature is linear for all materials tested. Fig. 2 shows a plot of thermal expansion coefficient versus composition. The largest thermal expansion coefficient occurs in the gadolinium-doped ceria and a slightly smaller value is observed for yttria stabilised zirconia. The effect of producing a composite material appears to be a decrease in thermal expansion coefficient relative to the pure cerium gadolinium oxide. The lowest thermal expansion coefficient was observed for the sample containing 30% doped ceria.

A typical complex plane plot for the samples is shown in Fig. 3. Bulk resistance is represented by the high frequency semicircle whilst the lower frequency semicircle represents the grain boundary resistance. The materials frequency response can be represented using an equivalent circuit diagram comprising of resistors and capacitors. An equivalent circuit for the composite electrolyte is given in Fig. 4. The resistor, R_e, represents electrode and lead resistance. Grain boundary response is represented by the resistor, R_{gb}, and capacitor, C_{gb}, and grain interiors by the resistor, R_{gi}, and capacitor,

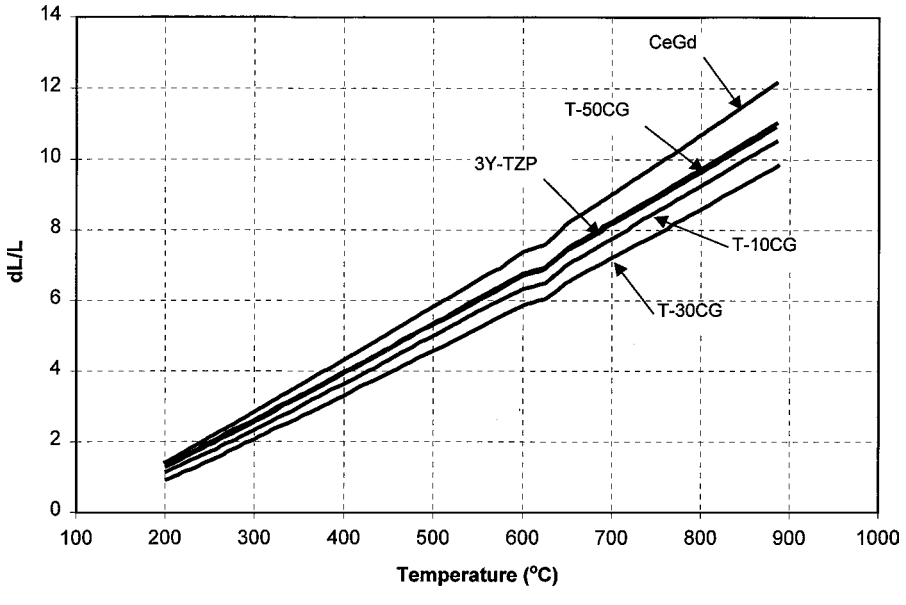

Figure 1 Thermal expansion ($\mathrm{d}L/L$) versus temperature.

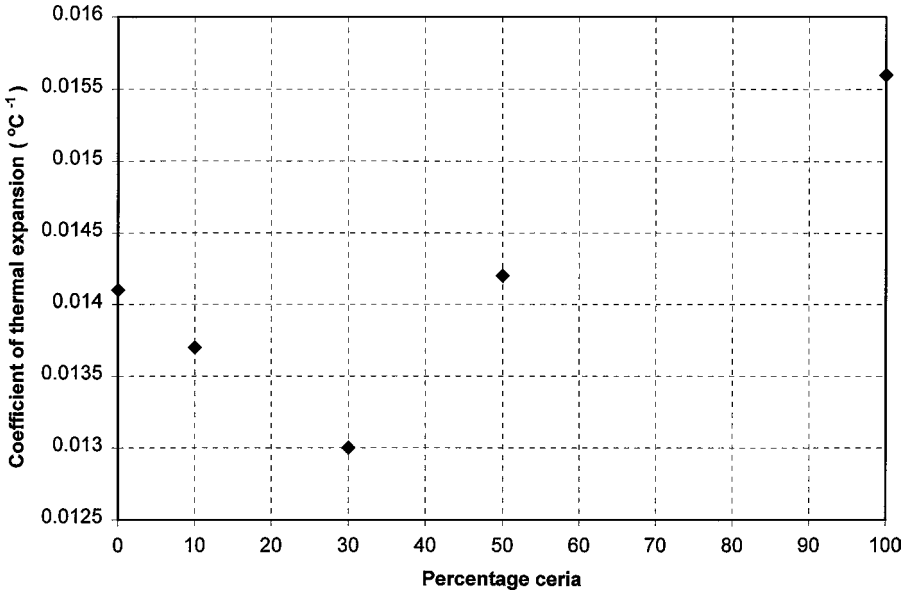

Figure 2 Coefficient of thermal expansion versus percentage ceria.

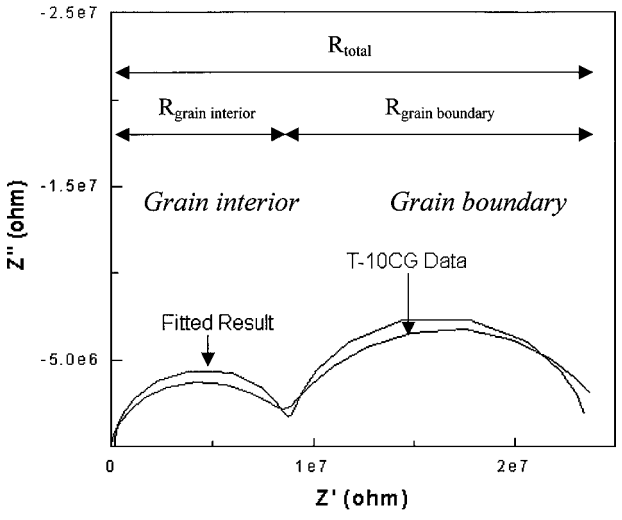

Figure 3 Typical complex plane plot for cerium gadolinium oxide/ zirconia composite.

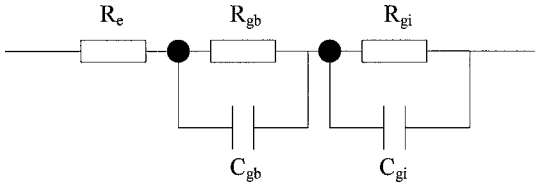

Figure 4 Equivalent circuit for frequency response of composite.

C_{gi}. Actual values of the resistors and capacitors in the model are dependant on sample properties and obtained by fitting a circle to the corresponding semicircle in the complex plane plot. Resistances obtained from the complex plane plots for each sample were used to calculate the total conductivity of the material as a function of temperature.

Plots of ln(conductivity $*$ T) versus $1000/T$ for the samples tested are shown in Fig. 5. The figure indicates an increase in conductivity with temperature as would be expected for ionically conducting materials. The conductivity of the cerium gadolinium oxide is higher than that of the zirconia. However, as gadolinia doped ceria is added to zirconia there is a gradual decrease in conductivity. This observation is also reflected in the activation energies shown in Table II.

TABLE II Activation energies calculated from impedance measurements

Sample	Activation energy, E_a (eV)
TZ3Y	0.96
T-10CG	0.99
T-30CG	1.02
T-50CG	1.06
CG	0.70

The relationship between conductivity and composition is given in Fig. 6, for a range of different temperatures between 200 and 500°C. The figure shows that the pure gadolinia doped ceria has a significantly greater conductivity when compared to pure yttria doped zirconia or the composite samples. A small decrease in conductivity is observed as the proportion of doped ceria in the sample increases. Conductivity is also inversely proportional to temperature.

The calculated activation energy for gadolinia doped ceria, 0.7 eV, is slightly lower than that reported in other literature of 0.92 eV [10]. The unexpected reduction in conductivity of the composite material can be attributed to two possible causes; the first could be the relatively high porosity of the material, typical density 93% and the second is the formation of a solid solution between the doped ceria and zirconia with a corresponding change in the intrinsic electrical properties.

Vegards law states that in a binary system forming a continuous series of solid solutions, the lattice parameters are linearly related to the atomic percentage of one of the components. The samples produced consist of four components, zirconia, ceria, gadolinia and yttria. However, the proportions of gadolinia and yttria are very small and for the purposes of this analysis it can

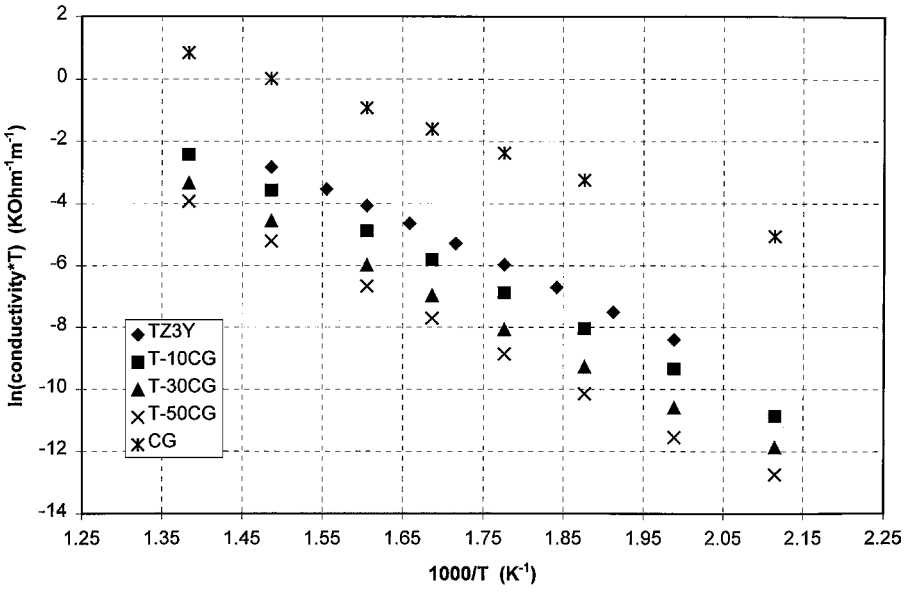

Figure 5 ln(conductivity $*$ T) versus $1000/T$.

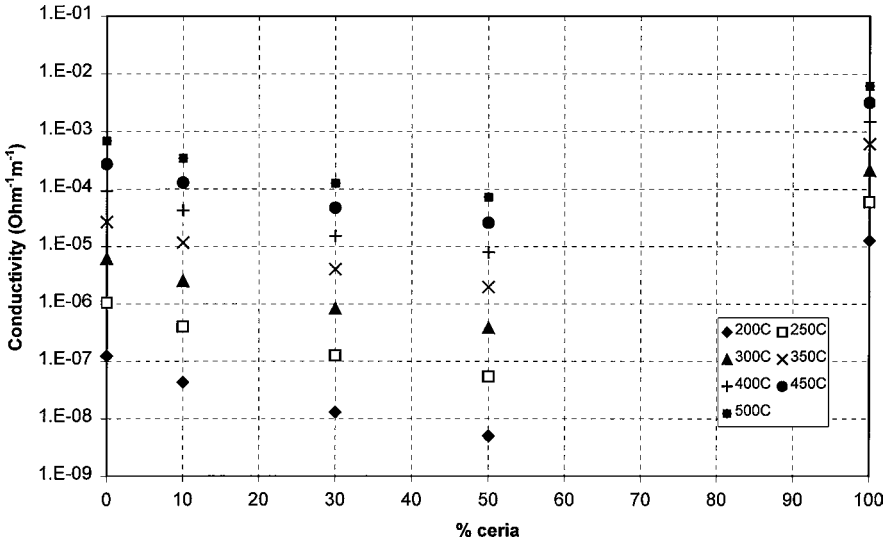

Figure 6 Conductivity versus percentage ceria in samples.

be assumed that the samples consist of a binary mixture of zirconia and ceria.

The X-ray diffraction patterns for each of the samples are shown in Fig. 7. The diffracting planes, which correspond to each of the peaks present in the zirconia and gadolinia doped ceria, are labelled in the figure. It is possible to see the disappearance of the cerium and gadolinium oxide peaks after addition to zirconia. This observation is particularly apparent for the cerium oxide (311) and gadolinium oxide (622) peaks. Both ceria and gadolinia have cubic structures, however the zirconia is tetragonal. It is likely that the addition of zirconia disrupts the cubic structure leading to the disappearance of the peaks. This would take place by the ceria and gadolinia forming a solid solution with zirconia.

As the proportion of gadolinia doped ceria added to the zirconia increases the position of the remaining zirconia peaks can be seen to move to a lower 2-theta value. This is particularly apparent in the peaks corresponding to the (111) and (200) planes. The 2-theta values of these peaks were used to calculate the lattice parameters for each sample. Plots of lattice parameter versus percentage zirconia are shown in Fig. 8. Linear regression lines plotted through the data indicate correlation coefficients of 0.90 and 0.93. This supports the suggestion that a solid solution is formed which follows Vegard's law. The increasing dimensions of the lattice parameter in the zirconia is caused by the relatively large ceria cations (Ce^{4+} = 0.87 Å) entering the lattice, substituting for the smaller zirconia ions (Zr^{4+} = 0.72 Å), (dimensions 6-fold coordination). The formation of a solid solution is the likely cause for the increase in activation energy of the composites compared to yttria stabilised zirconia and gadolinia doped ceria.

A disadvantage of using doped ceria as an electrolyte is its susceptibility to reduction in the presence of the low partical pressures of oxygen found in the fuel cell.

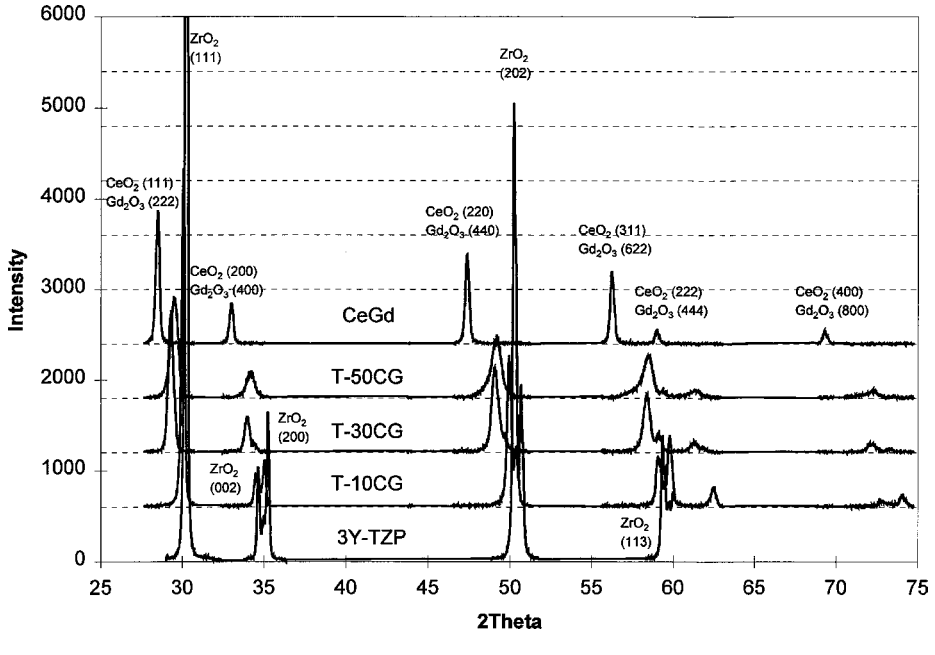

Figure 7 X-ray diffractions patterns for samples tested.

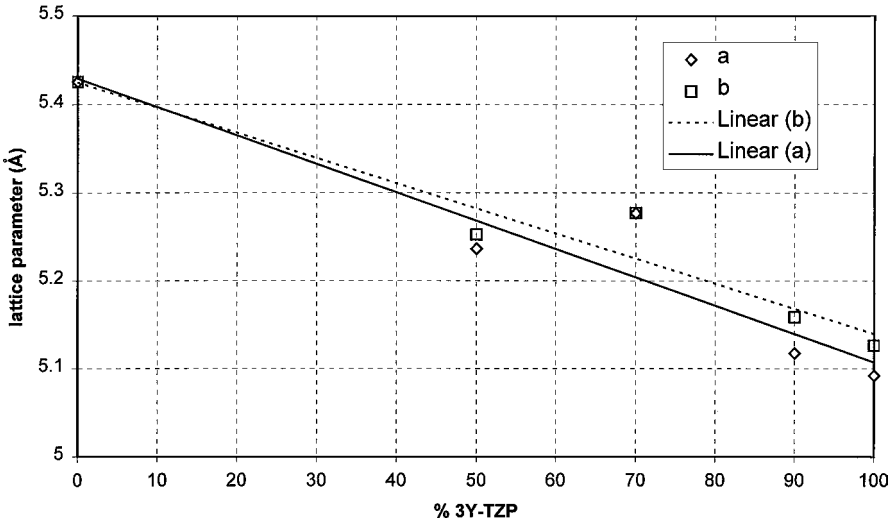

Figure 8 Lattice parameters, a and b calculated from (111) and (200) zirconia peaks, versus percentage zirconia contained within CeGd/YSZ composite electrolyte.

This leads to the reaction described in Equation 5.

$$2O^{2-} \leftrightarrow O_2 + 4e^- \quad (5)$$

The occurance of this reaction leads to an increase in the electronic transport number, and thus electronic conductivity. Electronic conductivity within the electrolyte can lead to passage of electrons between the anode and cathode and subsequent reduction in cell efficiency. Methods adopted to combat this problem include the application of a thin layer of zirconia to the electrolyte layer's surface to block electron flow, or a lowering of the fuel cell operating temperature to a level where the electronic conduction is insignificant.

4. Conclusions

Cerium gadolinium oxide—zirconia composites have been fabricated by conventional ceramic processing techniques with densities up to 93% of the theoretical density being attained. Addition of cerium gadolinium oxide to yttria stabilised zirconia in the range of 10–50% results in a decrease in ionic conductivity and activation energy, which can be attributed to the formation of a solid solution, as observed using XRD.

References

1. LARMINE DICKS, "Fuel Cell Systems Explained" (John Wiley & Sons, 2000) p. 166.
2. J. P. P. HUIJSMANS, *Curr. Opin. Solid State Mater. Sci.* **5** (2001) 317.
3. N. GFDS BONANOS, R. K. SLOTWINSKI, B. C. H. STEELE and E. P. BUTLER, *J. Mater. Sci. Lett.* **3** (1984) 245.
4. ISHITSUKA MASAYUKI, SATO TSUGIO, ENDO TADASHI and SHIMADA MASAHIKO, *J. Amer. Ceram. Soc.* **73**(8) (1990) 2523.
5. N. SAMMES *et al.*, *Denki Kagaku* **64** (1996) 674.
6. H. YAHIRO *et al.*, *J. Appl. Electrochem.* **18** (1988) 527.
7. J. E. BAUERLE, *J. Phys. Chem. Solids* **30** (1969) 2657.
8. J. R. MACDONALD and W. B. JOHNSON, in "Fundamentals of Impedance Spectroscopy-Impedance Spectroscopy: Emphasizing Solid Materials and Systems," edited by J. R. MacDonald (John Wiley & Sons, Inc., 1987) p. 1.
9. J. A. KILNER and R. J. BROOK, *Solid State Ion.* **6** (1982) 237.
10. SEONG JAE HONG *et al.*, *J. Electrochem. Soc.* **145**(2) (1998).

Received 18 October 2002
and accepted 18 August 2003